Journal of the Serbian Chemical Society
JSCS-info@shd.org.rs • www.shd.org.rs/JSCS
J. Serb. Chem. Soc. *83* (7–8) 837–846 (2018)
JSCS–5116
UDC 519.677+66.095.252.091.7:
547.313.2/.3:541.571.3
Original scientific paper

A DFT investigation of the Diels–Alder reaction of ethyl propiolate to the cage-annulated hexacyclo[7.5.2.$0^{1,6}$.$0^{6,13}$.$0^{8,12}$.$0^{10,14}$]-hexadeca-2,4-diene-7,16-dione

ABDURRAHMAN ATALAY and RIZA ABBASOGLU*

Department of Chemistry, Karadeniz Technical University, 61080 Trabzon, Turkey

(Received 13 November 2017, revised 3 March, accepted 5 March 2018)

Abstract: The Diels–Alder (DA) reaction between the cage-annulated diene hexacyclo[7.5.2.$0^{1,6}$.$0^{6,13}$.$0^{8,12}$.$0^{10,14}$]hexadeca-2,4-diene-7,16-dione (HHDD) with a cyclohexa-1,3-diene moiety and ethyl propiolate (EP) dienophile was investigated by the DFT method at the B3LYP/6-31+G(d,p) level to elucidate the mechanism and regioselectivity features of the reaction. The geometrical and electronic structures of the caged diene HHDD and EP were studied at B3LYP/6-31+G(d,p) level. In order to identify facial- and regio-selectivity of the DA reaction of HHDD and EP, the frontier molecular orbital (FMO) interactions of the reactants according to the FMO theory, and the molecular electrostatic potential map of HHDD were examined. The potential energy surface (PES) of the related DA reaction was calculated, and optimizations of transition states and of products corresponding to critical points on the PES were performed at the B3LYP/6-31+G(d,p), and their configurations were determined. In addition, the thermodynamic and kinetic parameters of each possible cycloaddition reaction were calculated using the B3LYP/6-31+G(d,p) method to determine whether the reaction occurs under thermodynamic or kinetic control. The thermochemical results showed that the related DA cycloaddition proceeds under kinetic control, and the activation energies of *syn* cycloadditions are clearly lower than that of *anti* cycloadditions. The theoretical calculations are in good agreement with experimental results.

Keywords: DFT calculations; Diels–Alder cycloadditions; cage-fused dienes; π-facial selectivity.

INTRODUCTION

The Diels–Alder (DA) reactions of cage compounds with facially differentiated 1,3-diene moieties have been the subjects of extensive studies in recent years.[1–8] Cage-fused cyclohexa-1,3-dienes are widely used for this type DA reactions as very useful substrates due to the absence of conformational uncer-

* Corresponding author. E-mail: rabbas@ktu.edu.tr
https://doi.org/10.2298/JSCJSC171113035A

tainties in its structures. Isolated cases of such reactions of some dienophiles with a π-facially differentiated cyclohexa-1,3-diene, *e.g.*, hexacyclo-[7.5.2.0^{1,6}.0^{6,13}.0^{8,12}.0^{10,14}]hexadeca-2,4-diene-7,16-dione (HHDD)[9] have been studied. Herein a related study of the DA cycloaddition reaction of ethyl propiolate (EP) to caged diene HHDD is reported. Experimental results showed that only P3 and P4 (product ratio 40:60, respectively)[9] stereoisomers of the four possible cycloadducts were obtained in this reaction (Fig. 1). These cycloadducts were formed by the attack of EP on the *syn*-π-face of HHDD. In order to scrutinize the facial- and regio-selectivity of the related reaction, the geometrical and electronic structures of the reactants were theoretically investigated. The presence of *syn*-π-facial selectivity in the reaction arises from the steric interactions between the hydrogens of the cyclobutane ring on the *anti* face of HHDD and the EP dienophile. Namely, the steric interactions in the attack of EP to the *anti*-π--face of HHDD result in unstable cycloadducts. Mutual orbital overlaps between the diene and the dienophile according to the frontier molecular orbital (FMO[10–15]) theory were calculated by the B3LYP/6-31+G(d,p) method to explore the reaction mechanism. The molecular electrostatic potential (MEP)[16,17] map of the cage diene HHDD were investigated at the B3LYP[18,19] level with the 6-31+G(d,p)[20] basis set to explain the selectivities of the reaction. Potential energy surface (PES) of this cycloaddition was computed by B3LYP/6-31+G(d,p), and the transition states and the products corresponding to the stationary points (saddle points and minima) were determined. Furthermore, the kinetic parameters (Δ*E**, Δ*H**, Δ*S** and Δ*G**) and thermodynamic parameters (Δ*E*, Δ*H*, Δ*S* and Δ*G*) for each cycloaddition were calculated at the B3LYP/6-31+G(d,p) level to determine the reaction pathway.

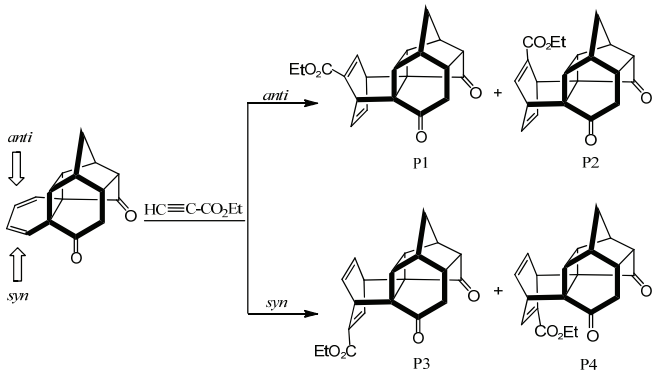

Fig. 1. Diels–Alder reaction between HHDD and EP.

COMPUTATIONAL METHODS

The DA reaction between HHDD and ethyl propiolate was investigated by the DFT/ /B3LYP method with the 6-31+G(d,p) basis set. The electronic structures of HHDD and EP

were investigated by the same method. The PES of the DA cycloaddition reactions were calculated at the B3LYP/6-31+G(d,p) level. All transition states with only one imaginary frequency and all reactants and products with all real frequencies were characterized. Intrinsic reaction coordinate (IRC)[21,22] calculations were performed to verify the association between reactants, transition states and products of each reaction pathway. Solvent effects were performed at same theory level with the 6-311++G(d,p) basis set and with a conductor-like polarizable continuum solvation model (CPCM)[23,24] (with UAKS cavities[25]) in toluene (ε = 2.38). Frequency calculations were performed by the B3LYP/6-31+G(d,p) method to obtain the thermochemistry parameters of each cycloaddition. All the calculations were performed with Gaussian 03.[26]

RESULTS AND DISCUSSION

The mutual interaction between the FMO orbitals of a diene and a dienohile in intermolecular DA reactions, which is either between the HOMO of the diene and the LUMO of the dienophile or the LUMO of the diene and the HOMO of the dienophile, could help to explain the reaction mechanism. According to the Klopman–Salem equation,[27,28] the smaller the HOMO–LUMO energy gap between the FMO orbitals of the reactants, the higher is the mutual overlap energy of the molecules, and the stronger is the overlapping of the orbitals.[29] In the present study, frontier molecular orbital interactions of the reactants were investigated by the B3LYP/6-31+G(d,p) method in order to explain the mechanism of the DA reaction between HHDD and EP. According to the theoretical results, favorable orbital overlapping was found to be between the HOMO orbital of the HHDD diene and the LUMO of the EP dienophile (Fig. 2). Namely, the related DA cycloaddition is controlled by $HOMO_{HHDD}$–$LUMO_{EP}$ interaction and is classified as a normal Diels–Alder reaction.

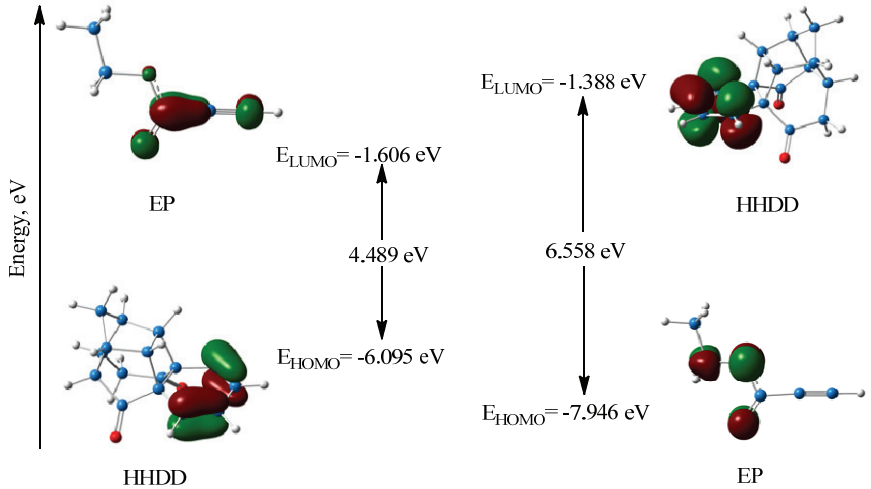

Fig. 2. FMO interaction diagrams, HOMO–LUMO gap energies of the reactants calculated by the B3LYP/6-31+G(d,p) method.

The molecular electrostatic potential (MEP) map is widely used to identify the most probable site of molecules for cycloaddition in intermolecular DA reactions.[30,31] The red on the map indicates the negative region pertaining to electrostatic potential, representing the region with a high electron density on the entire molecule, which is hence prone to cycloaddition. The blue indicates the region with partially positive charges, and this site is unfavorable for cycloaddition. In order to identify the reaction-prone site of the caged diene HHDD, the MEP map of the molecule was obtained from its geometry optimized by the B3LYP/6--31+G(d,p) method. As can be seen from computed MEP map, the reaction-prone site of HHDD (more red) for cycloaddition is on its *syn*-π face (Fig. 3). The reason for more red on the *syn*-face of the molecule is due to both the presence of carbonyl substituents on *syn*-face of HHDD and there being more electron density on the *syn*-face compared to that of on the *anti*-face of HHDD.

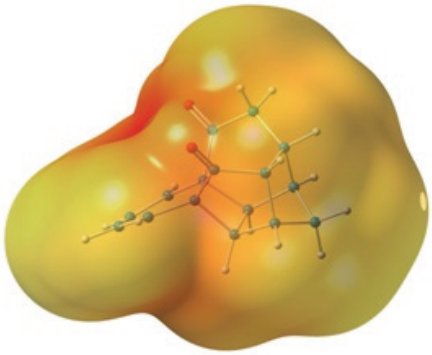

Fig. 3. MEP map of HHDD.

In order to better explain the mechanism of the related DA reaction, the geometries of the transition states of the reaction corresponding to stationary points on PES were optimized by the HF/3-21G, HF/6-31*, B3LYP/6-31G(d) and B3LYP/6-31+G(d,p) methods in the gas phase and their structures and stabilities were compared with each other (Fig. 4 and Table I). According to the calculated relative energies of transition states, the TS4 and TS3 transition states are clearly more stable than the TS1 and TS2 ones. Additionally, the most stable transition state, TS4, is energetically 0.589 (at B3LYP/6-31+G(d,p) level) and 0.788 kcal* mol^{-1} (at HF/6-31G*) lower than TS3 (Table I).

The bond formation length and bond order are used to gain an insight into bond formation or bond breaking in a chemical reaction. The bond formation lengths and bond orders (in parenthesis) in the transition states of the DA reaction between HHDD and EP are shown in Fig. 4 and given in Table II. In TS3 and TS4 transition states, the C(14)–C(29) and C(15)–C(30) bond formation lengths were calculated at B3LYP/6-31+G(d,p) level as 2.193–2.418 Å and 2.297–2.292

* 1 kcal = 4184 J

Å, respectively, and the bond orders were calculated as 0.192–0.133 and 0.157––0.168, respectively. This information also indicates that the C(14)–C(29) and C(15)–C(30) in TS4 are more advanced than that in the TS3 transition state for bond formation. It could also be stated that when all the transition states are compared in terms of bond formation length and bond order, this DA cycloaddition would proceeds on the *syn*-π face of HHDD.

TABLE I. Relative energies (kcal mol^{-1}) of the transition states

Transition state	Method			
	HF/3-21G	HF/6-31G*	B3LYP/6-31G(d)	B3LYP/6-31+G(d,p)
TS1	10.217	8.523	6.271	5.886
TS2	8.407	5.474	2.990	2.548
TS3	1.204	0.788	0.363	0.589
TS4	0	0	0	0

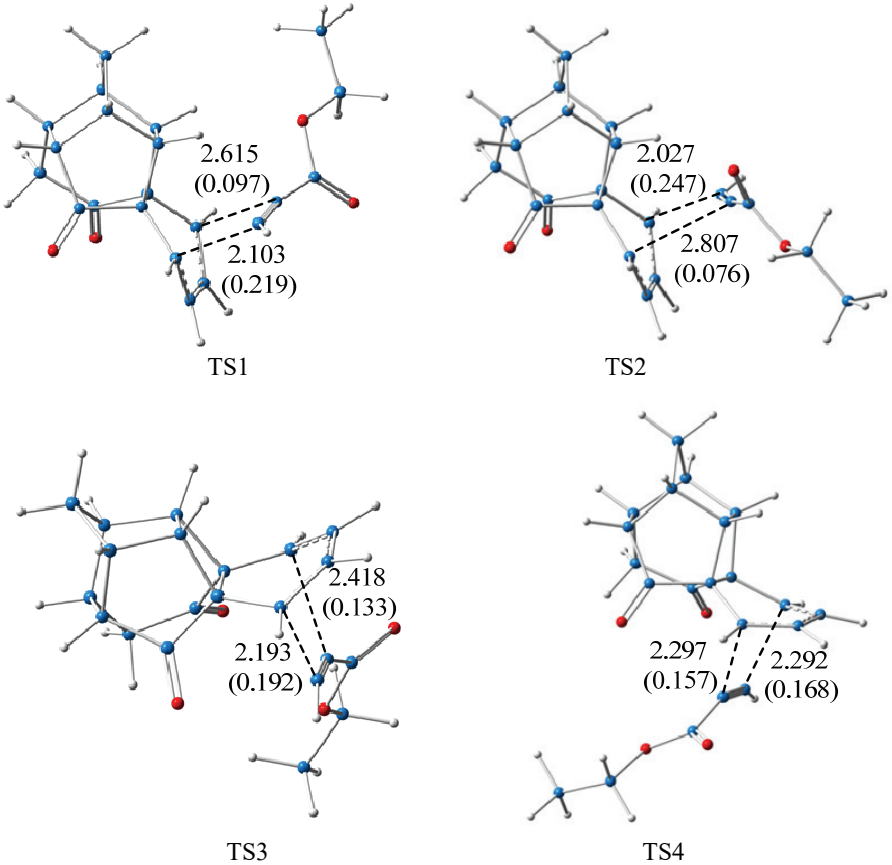

Fig. 4. Optimized geometries of transition states (at B3LYP/6-31+G(d,p) level). Bond formation lengths in Å, bond orders in parenthesis.

Kinetic parameters of each DA cycloaddition were calculated using the B3LYP/6-31+G(d,p) method. According to the theoretical results, the *syn*-cycloadditions (TS3 and TS4) have the lowest activation energies. The lowest activation Gibbs energy change (ΔG^*) and activation enthalpy change (ΔH^*) are also found for the *syn*-cycloadditions (see Table III), so this DA reaction proceeds *via* TS4 transition states.

TABLE II. Bond formation lengths (Å) and bond orders of transition states (at the B3LYP/6--31+G(d,p) level)

Property		Transition state			
		TS1	TS2	TS3	TS4
Bond length	$r_{C(14)-C(27)}$	2.103	2.807	–	–
	$r_{C(15)-C(28)}$	2.615	2.027	–	–
	$r_{C(14)-C(29)}$	–	–	2.193	2.297
	$r_{C(15)-C(30)}$	–	–	2.418	2.292
Bond order	C(14)–C(27)	0.219	0.076	–	–
	C(15)–C(28)	0.097	0.247	–	–
	C(14)–C(29)	–	–	0.192	0.157
	C(15)–C(30)	–	–	0.133	0.168

TABLE III. Kinetic parameters of DA cycloaddition between HHDD and EP (B3LYP/6--31+G(d,p))

Transition state	ΔE^* / kcal mol^{-1}	ΔH^* / kcal mol^{-1}	ΔS^* / cal mol^{-1} K^{-1}	ΔG^* / kcal mol^{-1}
TS1	29.711	29.119	43.475	42.081
TS2	26.499	25.902	44.724	39.209
TS3	24.474	23.877	46.501	37.715
TS4	23.885	23.293	46.260	37.086

The geometries of cycloadducts of each DA reaction between HHDD and EP corresponding to minima on PES were also optimized at the HF/3-21G, HF/6--31*, B3LYP/6-31G(d) and B3LYP/6-31+G(d,p) methods in gas phase, Fig. 5 and Table IV. According to the calculated relative energies of the cycloadducts, the relative energies of the cycloadducts (P1 and P2) of the *anti*-cycloadditions are lower than those of the cycloadducts (P3 and P4) of the *syn*-cycloadditions.

The thermodynamic parameters for each DA cycloaddition were calculated by the B3LYP/6-31+G(d,p) method (Table V). According to the results of the theoretical calculations, the *anti*-cycloadditions (P1 and P2) have the lowest reaction energies and enthalpies. Namely, *anti*-cycloadditions have favorable thermodynamic values for the cycloaddition but the reactions with the lowest activation energies are in *syn*-cycloadditions (Fig. 6). Therefore, this DA cycloaddition occurs from the *syn*-face of HHDD under kinetic control. In addition, these theoretical results are consistent with the experimental results.

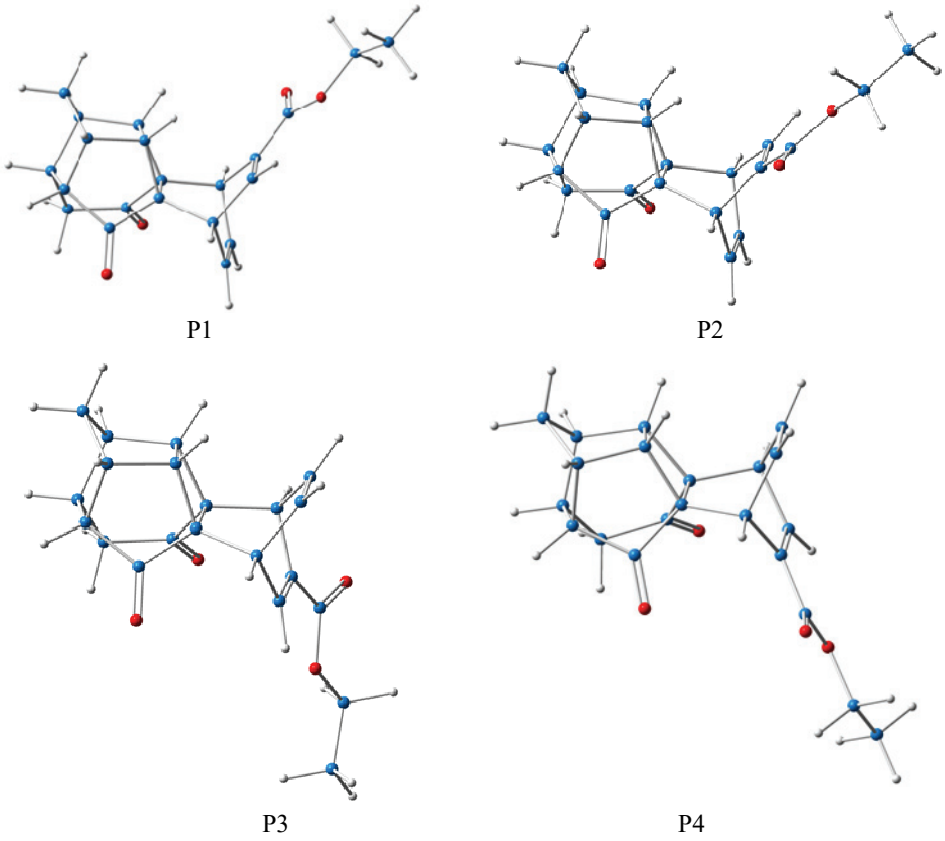

Fig. 5. Optimized geometries of the products (at the B3LYP/6-31+G(d,p) level).

TABLE IV. Relative energies (kcal mol^{-1}) of the products

Product	Method			
	HF/3-21G	HF/6-31G*	B3LYP/6-31G*	B3LYP/6-31+G(d,p)
P1	0.041	0.038	0.058	0.124
P2	0	0	0	0
P3	1.589	1.480	1.532	1.819
P4	0.418	0.403	0.499	0.774

TABLE V. Thermodynamic parameters for the DA cycloaddition between HHDD and EP (B3LYP/6-31+G(d,p))

Product	ΔE / kcal mol^{-1}	ΔH / kcal mol^{-1}	ΔS / cal mol^{-1} K^{-1}	ΔG / kcal mol^{-1}
P1	–40.824	–41.416	–51.856	–25.956
P2	–40.917	–41.509	–51.900	–26.035
P3	–39.199	–39.792	–53.196	–23.932
P4	–40.204	–40.796	–52.536	–25.132

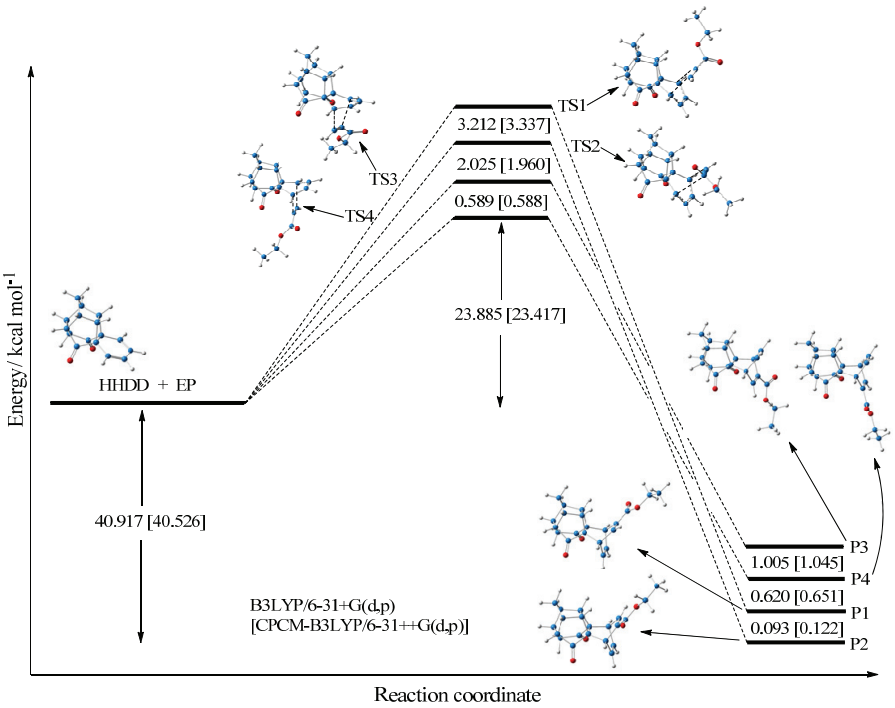

Fig. 6. The potential energy diagram for the DA reaction of EP to HHDD.

CONCLUSIONS

The DA cycloaddition reaction between the HHDD diene and the EP dienophile was theoretically investigated using the DFT method at the B3LYP level. The mutual overlapping of the frontier orbitals was found to occur between the HOMO of the HHDD diene and the LUMO of the EP dienophile according to the FMO theory as well as based on Klopmann–Salem equation. The MEP surface of the HHDD diene was also examined, and the chemically favorable reactive region of the molecule for cycloaddition was found to be its *syn*–π face. The DA cycloaddition is *syn*-face selective. The PES of the cycloaddition reactions was calculated, and the configurations of the transition states corresponding to stationary points on the PES were identified. The most stable transition state is energetically TS4. The calculated kinetic and thermodynamic parameters for each reaction pathway showed that activation energies of *syn* cycloaddition reactions, TS4 (23.885 kcal mol^{-1}) and TS3 (24.474 kcal mol^{-1}), were lower than those of the *anti* cycloadditions, and reaction energies of *anti* cycloadditions, P1 (–40.824 kcal mol^{-1}) and P2 (–40.917 kcal mol^{-1}), were the lowest values. Therefore, the DA cycloaddition reaction of HHDD and EP theoretically proceeds on the TS4 pathway under kinetic control, and the *syn* cycloadducts are the

favorable products. The results of all theoretical calculations were in good agreement with experimental results.

ИЗВОД

DFT ИСТРАЖИВАЊЕ ДИЛС–АЛДЕРОВЕ РЕАКЦИЈЕ ЕТИЛ-ПРОПИОЛАТА НА ПРСТЕНАСТО–КАВЕЗАСТИ ХЕКСАЦИКЛО[7.5.2.$0^{1,6}$.$0^{6,13}$.$0^{8,12}$.$0^{10,14}$]ХЕКСАДЕКА--2,4-ДИЕН-7,16-ДИОН

ABDURRAHMAN ATALAY и RIZA ABBASOGLU

Department of Chemistry, Karadeniz Technical University, 61080 Trabzon, Turkey

Дилс–Алдерова (DA) реакција између прстенасто-кавезастог диена хексацикло–[7.5.2.$0^{1,6}$.$0^{6,13}$.$0^{8,12}$.$0^{10,14}$]хексадека-2,4-диен-7,16-диона (HHDD) који садржи циклохекса-1,3-диенски фрагмент, са етил-пропиолатном (EP) као диенофилом истраживана је путем DFT методе на B3LYP/6-31+G(d,p) нивоу како би се разјаснио механизам и региоселективне особине реакције. Геометријске и електронске структуре кавезастог диена HHDD и EP проучаване су на B3LYP/6-31+G(d,p) нивоу. Да би се идентификовала фацијална селективност и регио-селективност DA реакције HHDD и EP, проучаване су интеракције граничних молекулских орбитала (FMO) реактаната на основу FMO теорије, и мапе молекулског електростатичког потенцијала HHDD. Површина потенцијалне енергије (PES) сродне DA реакције је израчуната, и урађене су оптимизације прелазних стања и производа који одговарају критичним тачкама на PES на B3LYP/6-31+G(d,p) нивоу, и одређене су њихове конфигурације. Поред тога, термодинамички и кинетички параметри сваке могуће циклоадиционе реакције израчунати су користећи B3LYP/6--31+G(d,p) метод да би се утврдило да ли се реакција дешава уз термодинамичку или кинетичку контролу. Термохемијски резултати су показали да је DA циклоадиција кинетички контролисана, и активационе енергије *syn* циклоадиција су ниже од оних код *anti* циклоадиција. Теоријска израчунавања се добро слажу са експерименталним резултатима.

(Примљено 13. новембра 2017, ревидирано 3. марта, прихваћено 5. марта 2018)

REFERENCES

1. T. C. Chou, P. C. Hong, Y. F. Wu, W. Y. Chang, C. T. Lin, *Tetrahedron* **52** (1996) 6325
2. G. Mehta, R. Uma, *Tetrahedron Lett.* **36** (1995) 4873
3. J. M. Coxon, S. T. Fong, D. Q. McDonald, P. J. Steel, *Tetrahedron Lett.* **34** (1993) 163
4. W. D. Fessner, C. Grund, H. Prinzbach, *Tetrahedron Lett.* **32** (1991) 5935
5. J. M. Coxon, R. G. A. R. Maclagan, D. Q. McDonald, P. J. Steel, *J. Org. Chem.* **56** (1991) 2542
6. J. M. Coxon, S. T. Fong, K. Lundie, D. Q. McDonald, P. J. Steel, A. P. Marchand, F. Zaragoza, U. R. Zope, D. Rajagopal, S. G. Bott, W. H. Watson, R. P. Kashyap, *Tetrahedron* **50** (1994) 13037
7. A. S. Kushner, *Tetrahedron Lett.* **12** (1971) 3275
8. B. Pandey, U. R. Zope, N. R. Ayyangar, *J. Chem. Soc., Chem. Commun*. **2** (1990) 107
9. a) A. P. Marchand, H. S. Chong, B. Ganguly, R. Shukla, E. Z. Dong, A. Hazlewood, T. D. Power, W. H. Watson, S. G. Bott, *Tetrahedron* **57** (2001) 8629; b) A. P. Marchand, H.-S. Chong, B. Ganguly, J. M. Coxon, *Croat. Chem. Acta* **73** (2000) 1027
10. L. Salem, *J. Am. Chem. Soc.* **90** (1968) 543
11. L. Salem, *J. Am. Chem. Soc.* **90** (1968) 553
12. K. Fukui, *Acc. Chem. Res.* **4** (1971) 57

13. K. N. Houk, *Acc. Chem. Res.* **8** (1975) 361
14. K. N. Houk, in *Pericyclic Reactions*, A. P. Marchand, R. E. Lehr, Eds., Academic Press, New York, 1977, Vol. 2, p. 181
15. K. Fukui, *Angew. Chem., Int. Ed.* **21** (1982) 801
16. D. G. Truhlar, A. J. Kuppermann, *J. Am. Chem. Soc.* **93** (1971) 1840
17. R. Bonaccorsi, E. Scrocco, J. Tomasi, *J. Chem. Phys.* **52** (1970) 5270
18. A. D. Becke, *J. Chem. Phys.* **98** (1993) 5648
19. C. Lee, W. Yang, R. G. Parr, *Phys. Rev., B* **37** (1988) 785
20. R. Krishnan, J. S. Binkley, R. Seeger, J. A. Pople, *J. Chem. Phys.* **72** (1980) 650
21. C. Gonzalez, H. B. Schlegel, *J. Chem. Phys.* **90** (1989) 2154
22. C. Gonzalez, H. B. Schlegel, *J. Phys. Chem.* **94** (2002) 5523
23. M. T. Cances, V. Mennucci, J. Tomasi, *J. Chem. Phys.* **107** (1997) 3032
24. S. Miertus, E. Scrocco, J. Tomasi, *Chem. Phys.* **55** (1981) 117
25. V. Barone, M. Cossi, J. Tomassi, *J. Chem. Phys.* **107** (1997) 3210
26. *Gaussian 03, Revision B.03*, Gaussian Inc., Pittsburgh PA, 2003
27. G. Klopman, *J. Am. Chem. Soc.* **90** (1968) 223
28. L. Fleming, *Frontier Orbitals and Organic Chemical Reactions*, Wiley, London, 1977
29. T. Lipinska, *Tetrahedron* **61** (2005) 8148
30. A. E. Hayden, J. de Chancie, A. H. George, M. Dai, M. Yu, S. J. Danishefsky, K. N. Houk, *J. Org. Chem.* **74** (2009) 6770
31. J. S. Murray, D. Yepes, P. Jaque, P. Politzer, *Comput. Theor. Chem.* **1053** (2015) 270.